Assignment 1
Yoichiro Dobashi (ESS 563)

1) Derivation highlights (Part B)

Here, the strain tensor is derived from the far-field terms of **u** in the homogeneous, isotropic, linear elastic space, and small displacement.

$$\varepsilon_{ij}^{(th)}(X,t) = \frac{1}{2}(\frac{\partial u_i}{\partial x_j} + \frac{\partial u_j}{\partial x_i})$$
$$u(X,t) = \frac{1}{4\pi\rho}(\frac{1}{\alpha^3 r} n\left(n^T \ddot{M}(t-tp)n\right) + \frac{1}{\beta^3 r}(I - nn^T)\ddot{M}(t-ts)n)$$
$$u_i = \frac{1}{4\pi\rho}(\frac{1}{\alpha^3 r} n_i n_j n_k \ddot{M_{jk}}(t-tp) + \frac{1}{\beta^3 r}\left(\delta_{ij} - n_i n_j\right)\ddot{M_{jk}}(t-ts)n_k$$

Under the assumption that the P contribution is irrotational, and rotation arises from S radiation and non-radiation/induction terms.

P wave component is

$$\frac{\partial u_i(P)}{\partial x_l} = \frac{1}{4\pi\rho\alpha^3}(\frac{\partial}{\partial x_l}\left(\frac{1}{r}\right) n_i n_j n_k \ddot{M_{jk}}(t-tp) + \frac{1}{r}\frac{\partial\left(n_i n_j n_k\right)}{\partial x_l}\ddot{M_{jk}}(t-tp) + \left(\frac{1}{r}\right) n_i n_j n_k \frac{\partial\left(\ddot{M_{jk}}(t-tp)\right)}{\partial x_l})$$
$$= \frac{1}{4\pi\rho\alpha^3}(-\frac{n_l}{r^2} n_i n_j n_k \ddot{M_{jk}}(t-tp) + \frac{1}{r^2}((\delta_{il} - n_i n_l)n_j n_k + (\delta_{jl} - n_j n_l)n_i n_k + (\delta_{kl} - n_k n_l)n_i n_j)\ddot{M_{jk}}(t-tp)$$
$$-\frac{n_l}{r\alpha} n_i n_j n_k \dddot{M_{jk}}(t-tp)$$

Far-field term of P wave is

$$-\frac{1}{4\pi\rho\alpha^4}\frac{n_l}{r} n_i n_j n_k \dddot{M_{jk}}(t-tp)$$

S wave component is

$$\frac{\partial u_i(S)}{\partial x_l}$$
$$= \frac{1}{4\pi\rho\beta^3}(\frac{\partial}{\partial x_l}\left(\frac{1}{r}\right)(\delta_{ij} - n_i n_j)\ddot{M_{jk}}(t-ts)n_k + \frac{1}{r}\frac{\partial\left((\delta_{ij} - n_i n_j\right)}{\partial x_l}\ddot{M_{jk}}(t-ts)n_k + \frac{1}{r}(\delta_{ij}$$
$$- n_i n_j)\frac{\partial\left(\ddot{M_{jk}}(t-ts)\right)}{\partial x_l})n_k + \frac{1}{r}(\delta_{ij} - n_i n_j)\ddot{M_{jk}}(t-ts)\frac{\partial(n_k)}{\partial x_l}$$
$$= \frac{1}{4\pi\rho\beta^3}(-\frac{n_l}{r^2}(\delta_{ij} - n_i n_j)\ddot{M_{jk}}(t-ts)n_k - \frac{1}{r^2}((\delta_{il} - n_i n_l)n_j + (\delta_{jl} - n_j n_l)n_i)\ \ddot{M_{jk}}(t-ts)) - \frac{n_l}{r\beta}(\delta_{ij}$$
$$- n_i n_j)\dddot{M_{jk}}(t-ts)n_k + \frac{1}{r^2}(\delta_{ij} - n_i n_j)\ddot{M_{jk}}(t-ts)((\delta_{kl} - n_k n_l))$$

Far-field term of S wave is

$$-\frac{1}{4\pi\rho\beta^4}\frac{n_l}{r}(\delta_{ij} - n_i n_j)\dddot{M_{jk}}(t-ts)n_k$$

Theoretical strain wavefield is;

$$\varepsilon_{ij}^{(th)}(X,t) = \frac{1}{2}\left(\frac{\partial u_i}{\partial x_j} + \frac{\partial u_j}{\partial x_i}\right)$$
$$= -\frac{1}{8\pi\rho r}\left[\frac{1}{\alpha^4}\left(n_i n_j + n_j n_i\right) n_k n_l \ddot{M}_{kl}(t-tp)\right.$$
$$\left.+\frac{1}{\beta^4}\left\{\left((\delta_{ik} - n_i n_k\right)\ddot{M}_{kl}(t-ts) n_l n_j + \left((\delta_{jk} - n_j n_k\right)\ddot{M}_{kl}(t-ts) n_l n_i\right\}\right]$$

Theoretical rotation wavefield is;

$$\Omega_{ij}^{(th)}(X,t) = \frac{1}{2}\left(\frac{\partial u_i}{\partial x_j} - \frac{\partial u_j}{\partial x_i}\right)$$
$$= -\frac{1}{8\pi\rho r}\left[\frac{1}{\alpha^4}\left(n_i n_j - n_j n_i\right) n_k n_l \ddot{M}_{kl}(t-tp)\right.$$
$$\left.+\frac{1}{\beta^4}\left\{\left((\delta_{ik} - n_i n_k\right)\ddot{M}_{kl}(t-ts) n_l n_j - \left((\delta_{jk} - n_j n_k\right)\ddot{M}_{kl}(t-ts) n_l n_i\right\}\right]$$

2) Three-component Seismograms

Source (0, 0, 3000), Mo: 1.0e16, fc 2.0, dt=0.08333 based on f_{Nyq}=3f_{Nyq}=6Hz

Record length T=25.44sec from T ≥6max(r/α,r/β)+5τ.

Station St1 (10000, 0, 0), St2 (0, 10000, 0), St3 (10000, 10000, 0), St4 (-10000, -10000, 0)

Surface Boundary Condition

Although the geometry of my point source and station is on the half-space ($z \geq 0$), wave reflection and the surface strain condition ($\sigma_{iz} = 0$) is not considered in my model.

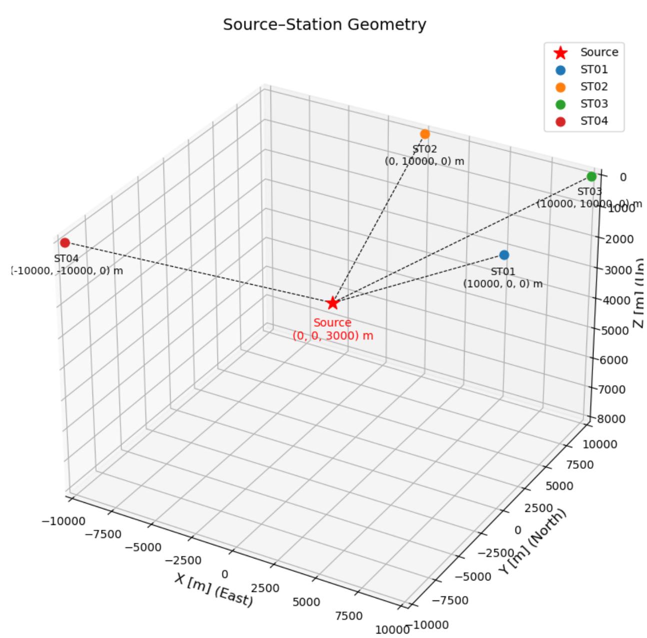

a) DC
Strike 135.0, Dip 20.0, Rake 90.0

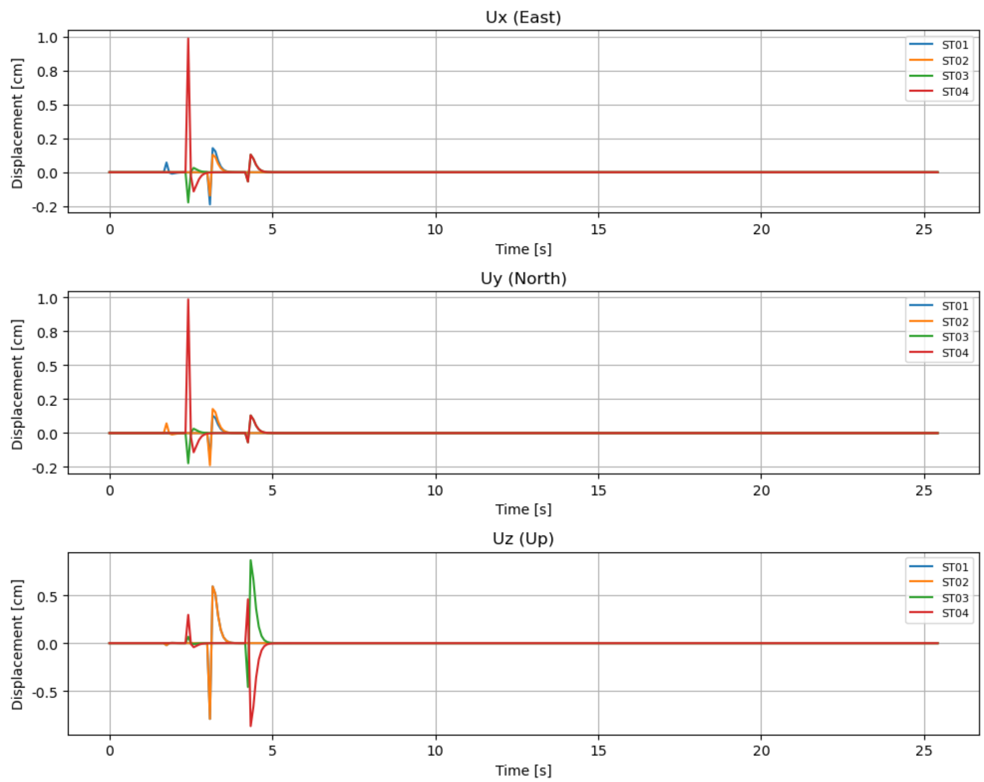

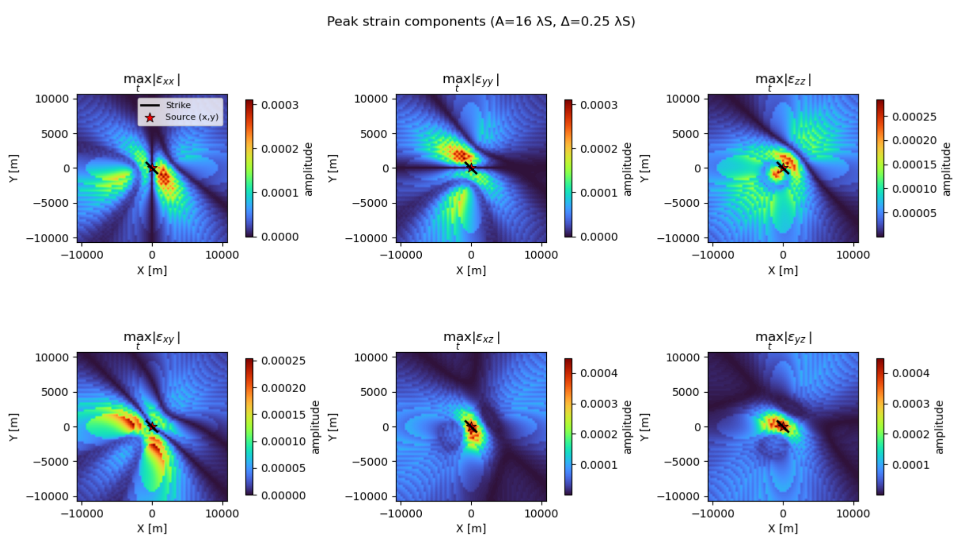

b) CLVD
Mxx = -0.3333, Myy = -0.3333, Mzz = 0.6667

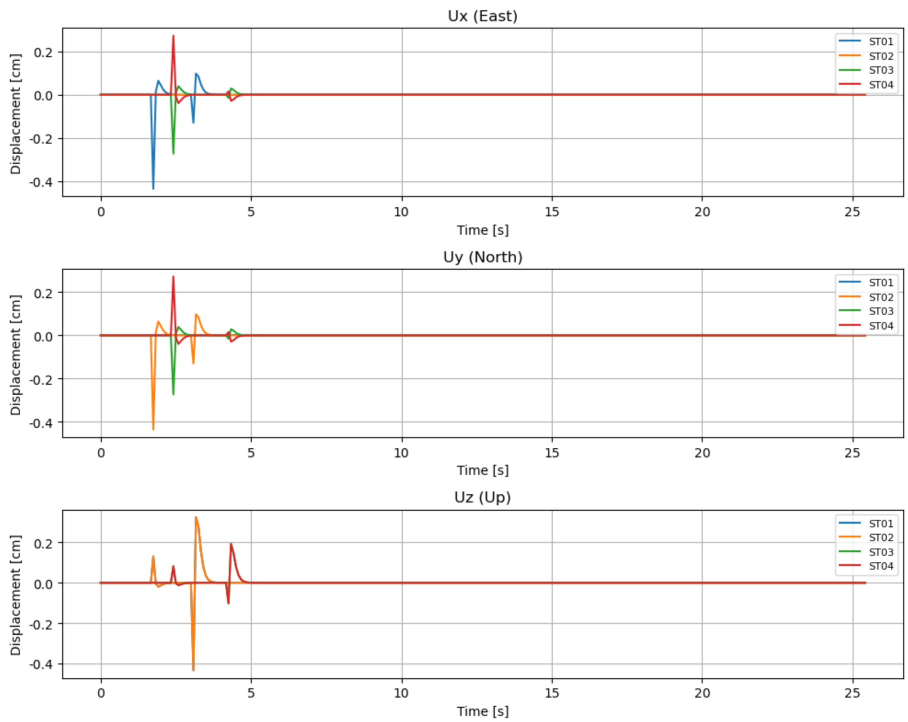

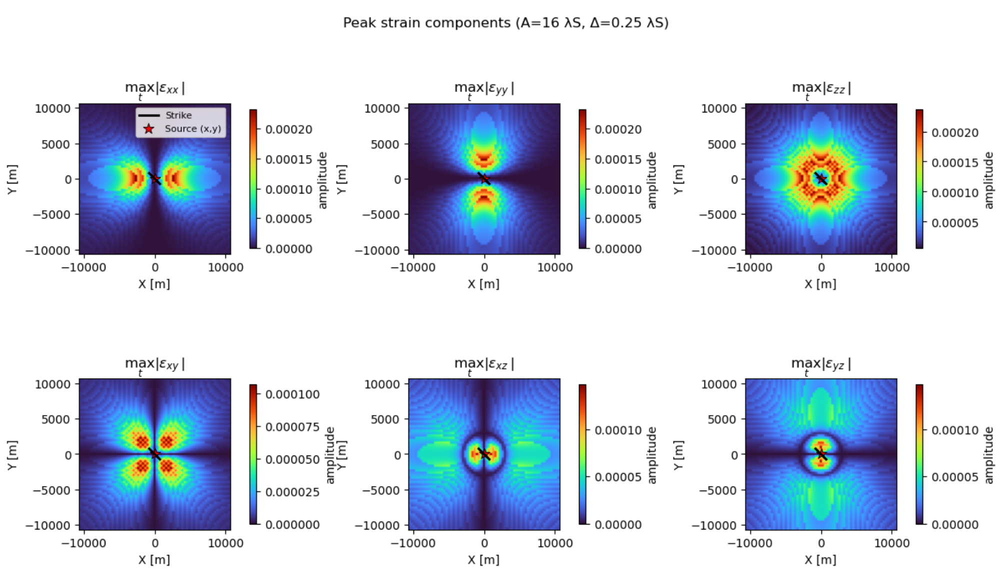

3) Theoretical vs. FD strain for selected stations

a) ST01

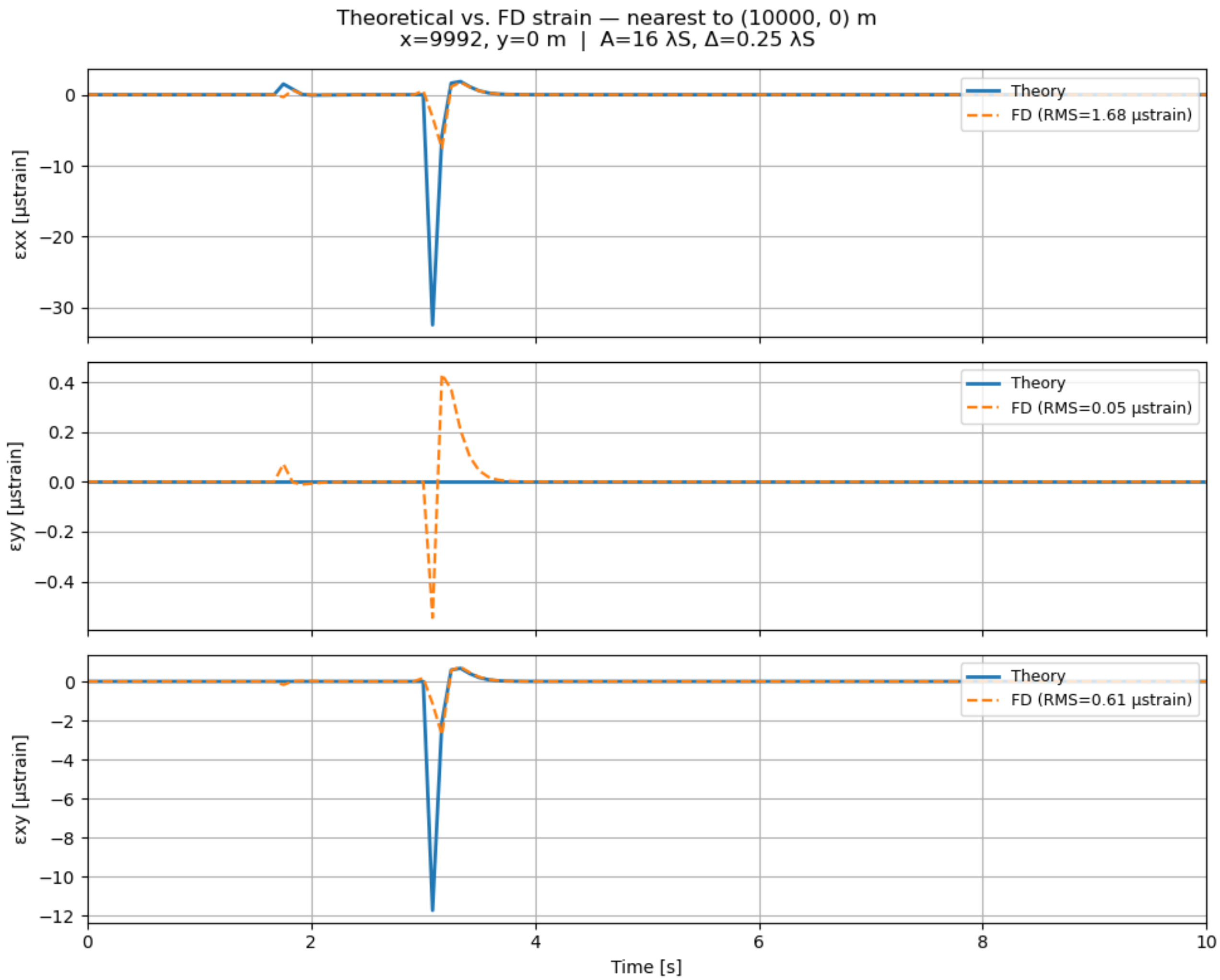

b) ST02

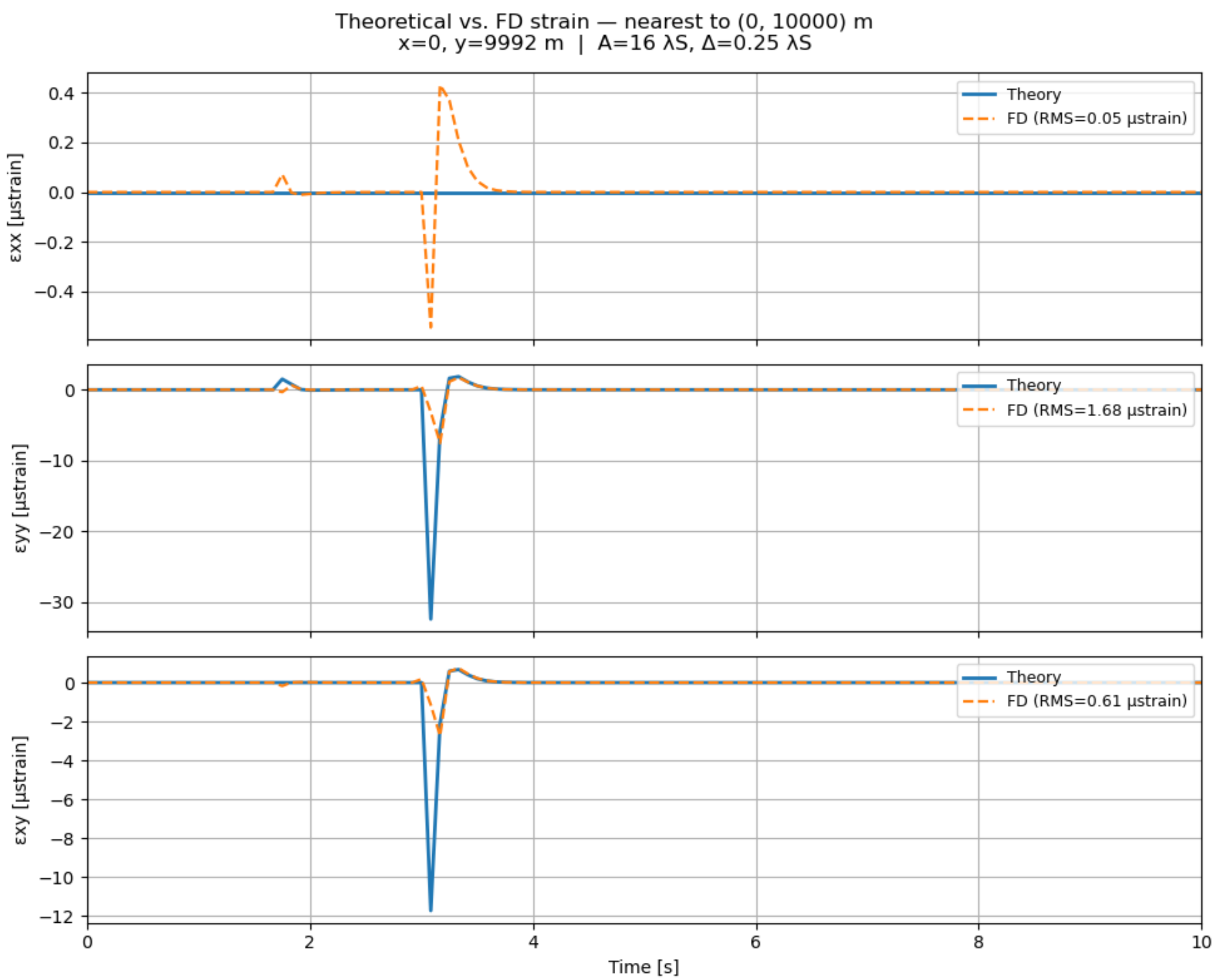
Theoretical vs. FD strain — nearest to (0, 10000) m
x=0, y=9992 m | A=16 λS, Δ=0.25 λS
Theory
FD (RMS=0.05 μstrain)
εxx [μstrain]
FD (RMS=1.68 μstrain)
εyy [μstrain]
FD (RMS=0.61 μstrain)
εxy [μstrain]
Time [s]

c) ST03

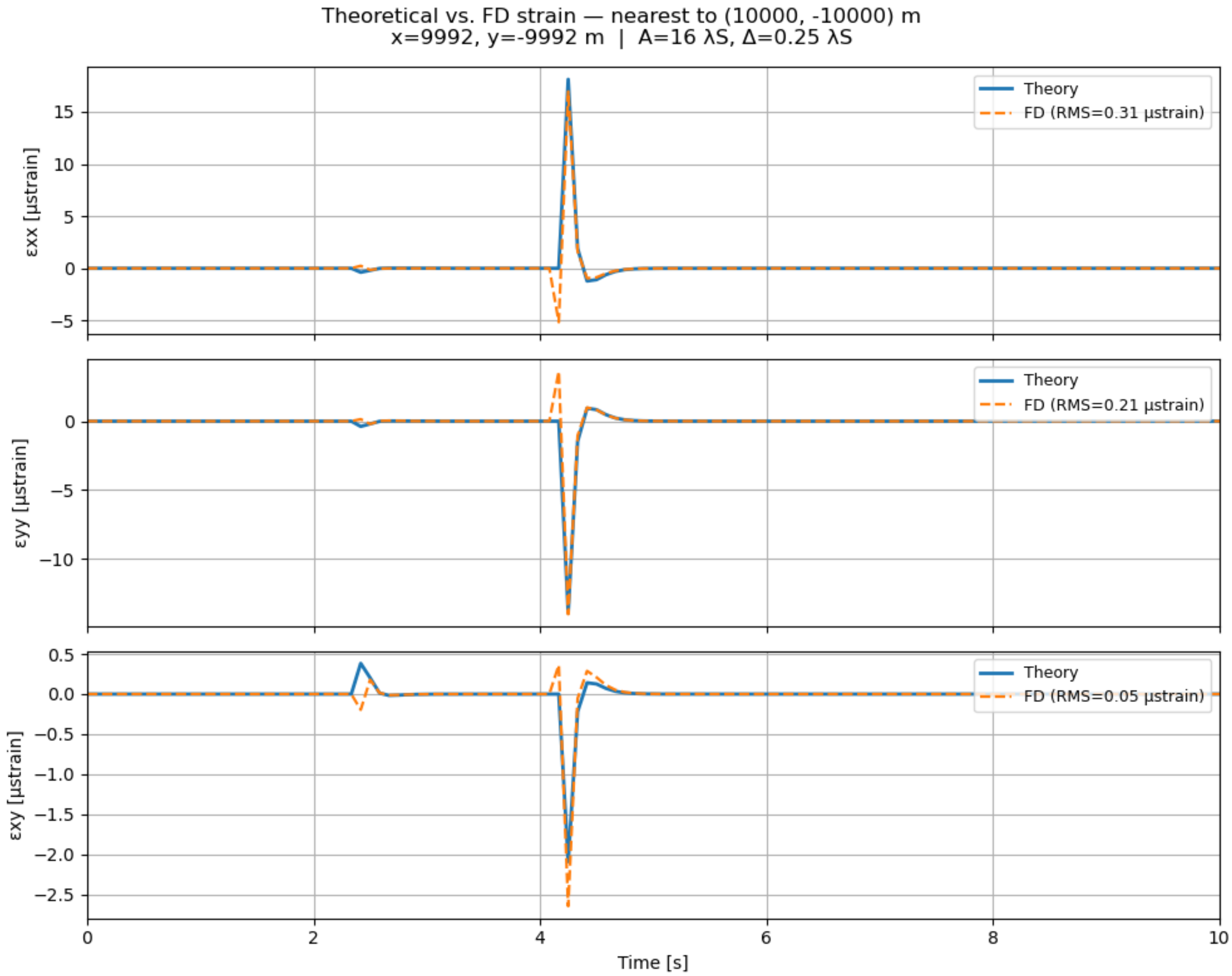
Theoretical vs. FD strain — nearest to (10000, -10000) m
x=9992, y=-9992 m | A=16 λS, Δ=0.25 λS
Theory
FD (RMS=0.31 μstrain)
εxx [μstrain]
Theory
FD (RMS=0.21 μstrain)
εyy [μstrain]
Theory
FD (RMS=0.05 μstrain)
εxy [μstrain]
Time [s]

4) ST04

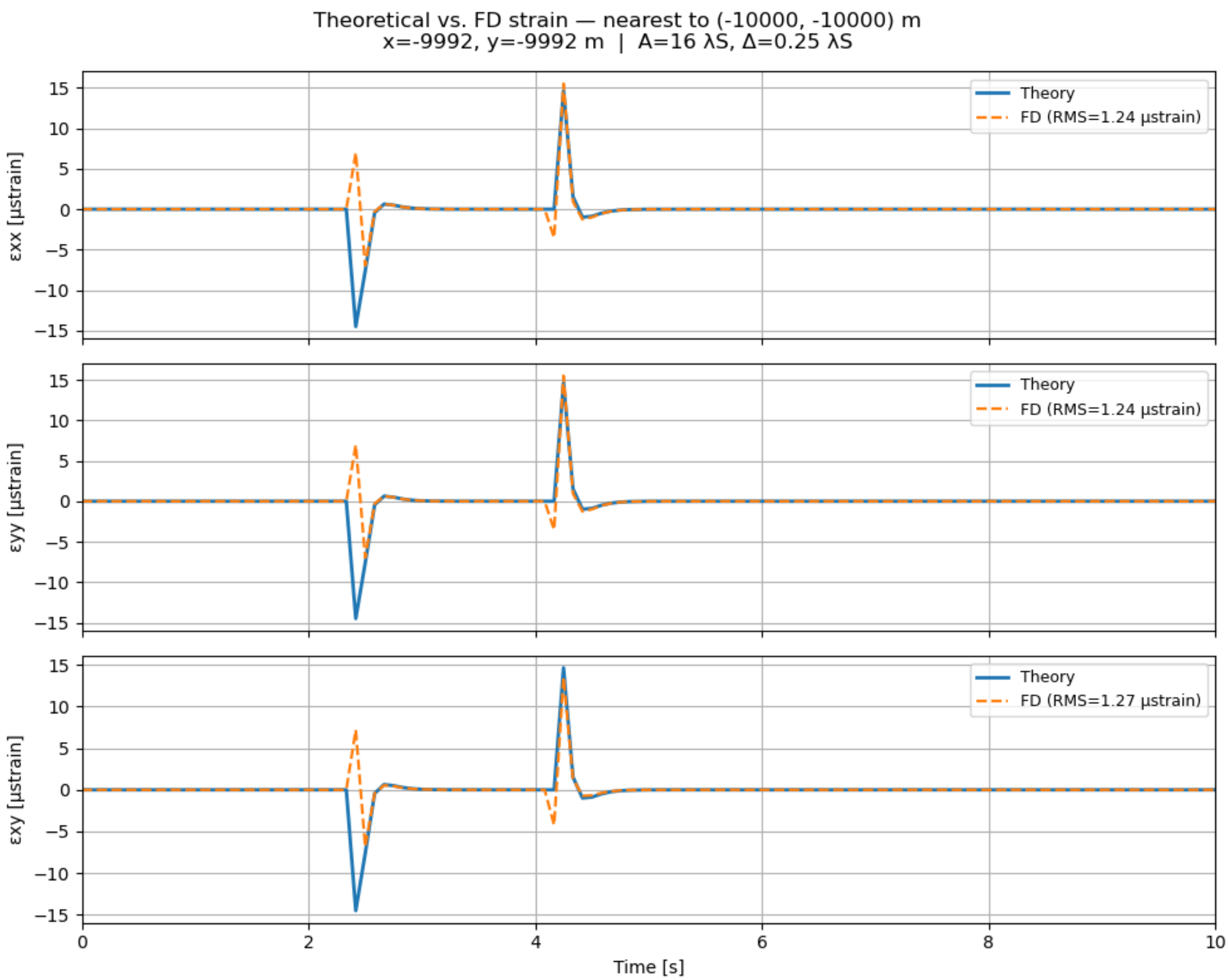

Theoretical vs. FD strain — nearest to (-10000, -10000) m
x=-9992, y=-9992 m | A=16 λS, Δ=0.25 λS
εxx [μstrain]
εyy [μstrain]
εxy [μstrain]
Theory
FD (RMS=1.24 μstrain)
Theory
FD (RMS=1.24 μstrain)
Theory
FD (RMS=1.27 μstrain)
Time [s]

5) MSE curves vs. Δ/λ_S and aperture, radiation patterns at the surface

a) MES curves

DC Strike 135.0, Dip 20.0, Rake 90.0

fc=2.0

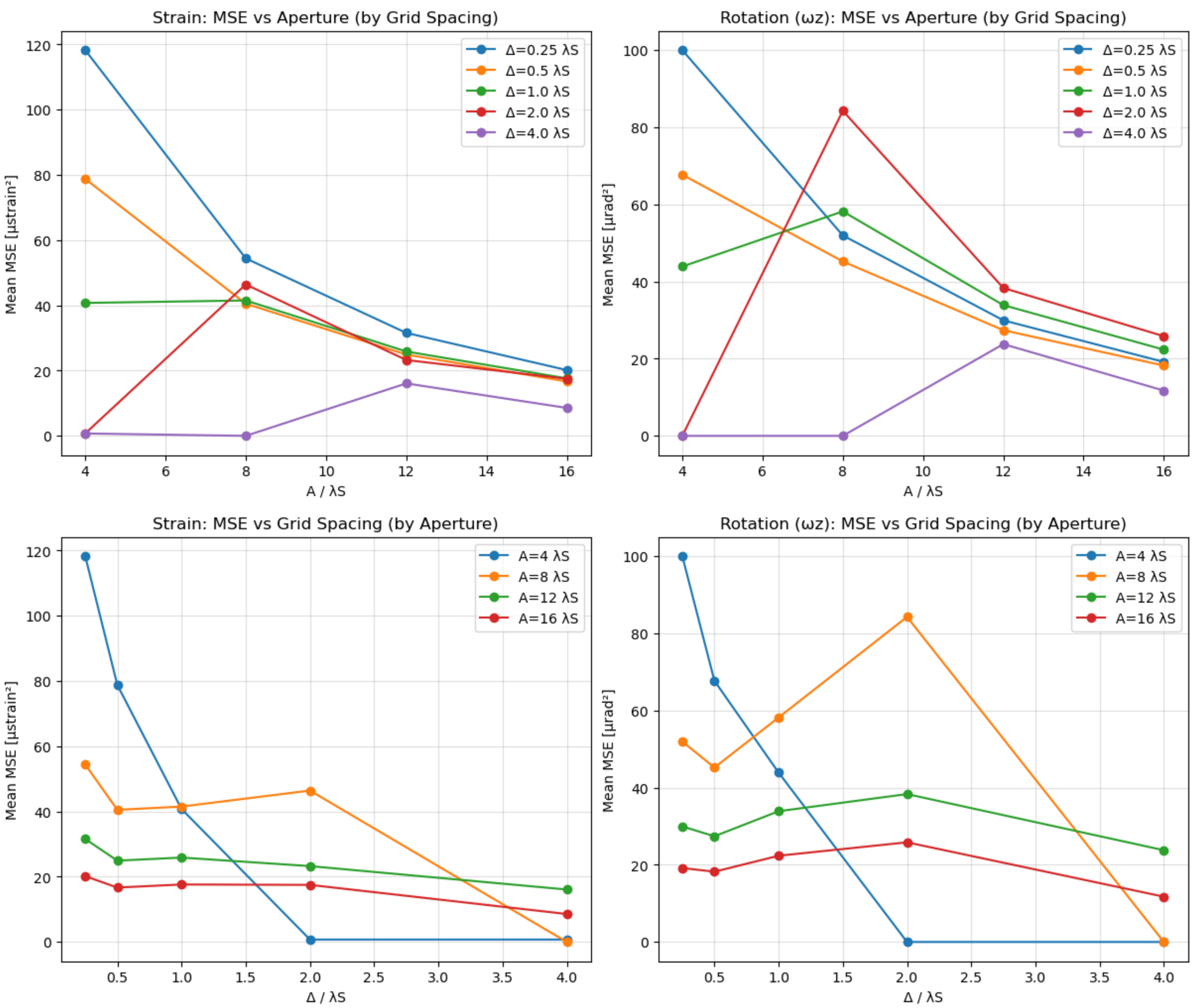

fc=1.0

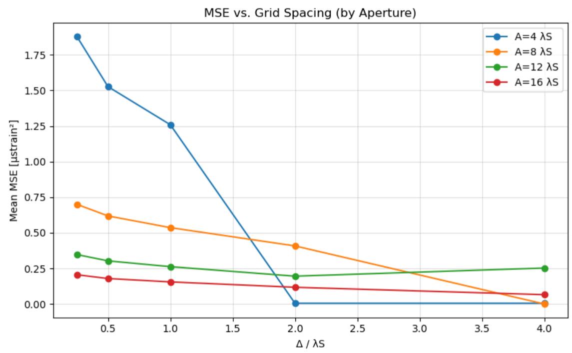

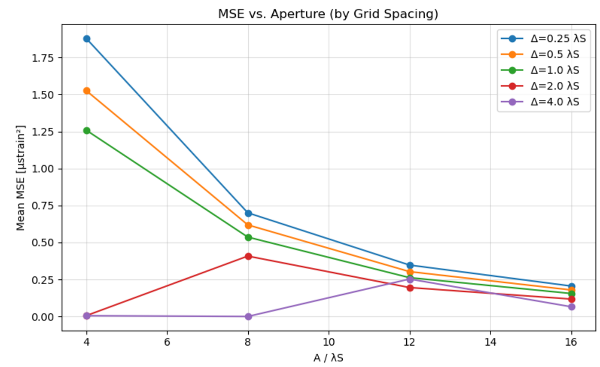

fc=4.0

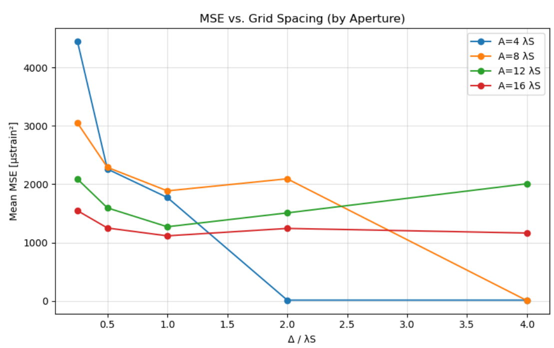

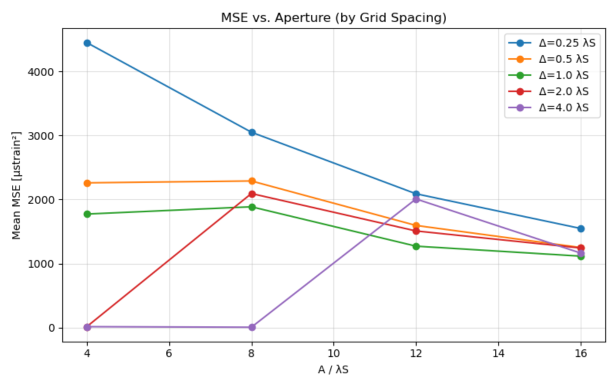

b) MES curves

DC Strike 135.0, Dip 90.0, Rake 0.0

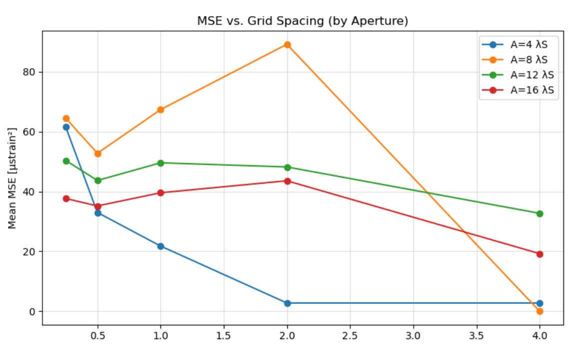

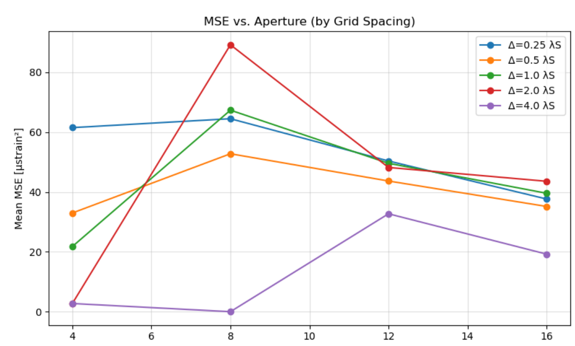

c) Radiation pattern

i) DC Strike slip

Strike 135.0, Dip 90.0, Rake 0.0

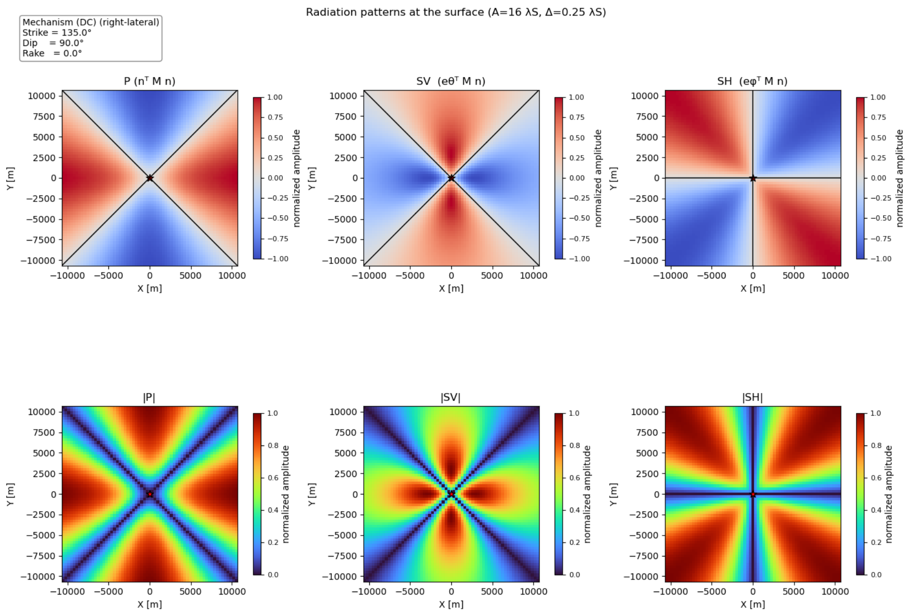

ii) DC

Strike 135.0, Dip 45.0, Rake 90.0

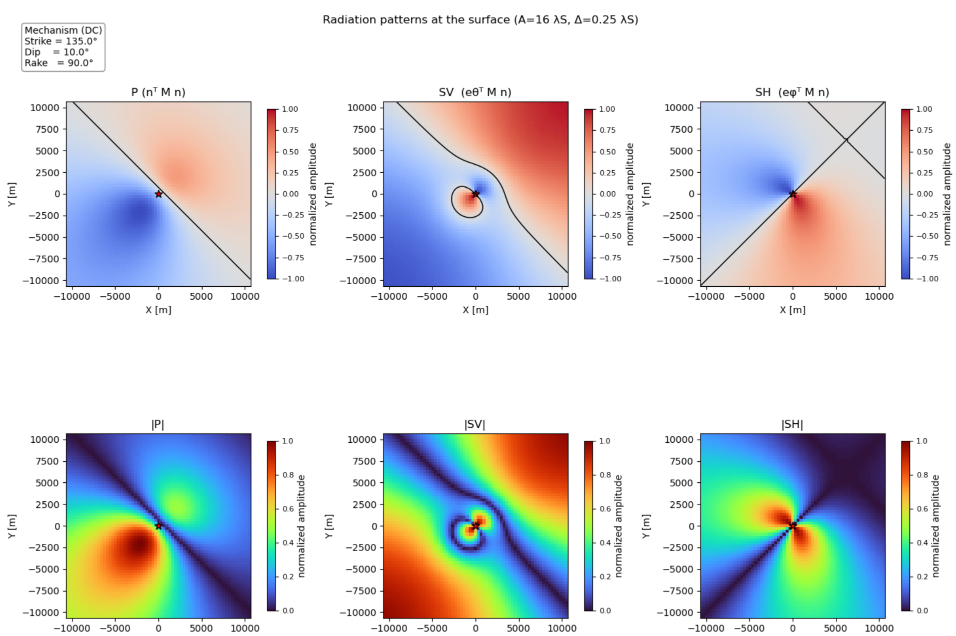

i) CLVD

Mxx=0.3333, Myy=0.3333, Mzz=0.9999

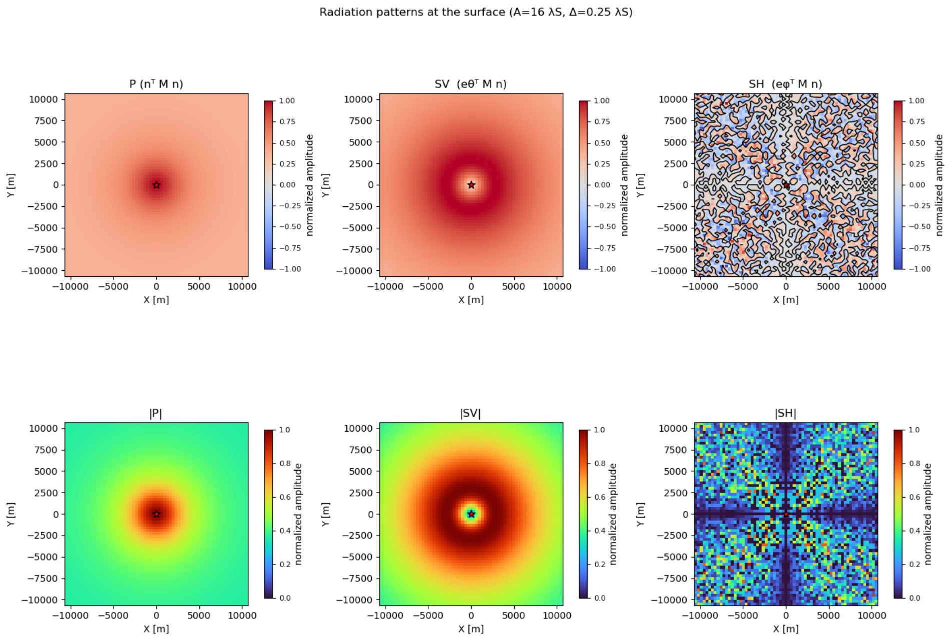

6) Discussion: Arrays as Wavefield-Gradient & Rotation Instrument (Part G)

a) How array spacing Δ and aperture A control accuracy/bandwidth of both strain and rotation estimates.
Array spacing Δ sets a resolution of high-wave number signal and control high frequency noise/bias coming from discretization scheme. Aperture sets low-wave number signal.
My result with fc=2.0sec, source depth 3km shows;

- Consistent MSE values when A/ λS is set to 12, 16 to both strain and rotation
- MSE has local minimum when Δ/λS is set to 0.5, and becomes large at 0.25
  Since Δ/λS=0.5 is Nyquist frequency, Δ/λS=0.25 is expected to have smaller MSE, however It doesn't be realized.

Thus, stations should be set as A/ λS ≥ 12, and Δ/ λS ≤ 0.5 with high frequency filtering.

b) Noise amplification in spatial differencing; filtering choices; sensitivity of ω vs. ε to high- wavenumber noise.
This test uses the centered-difference method, whose truncation error is dominated by the $u^{(3)}(x)$term. Consequently, high-frequency content and sharp peaks can greatly amplify the error.

$$\frac{u(x+\Delta)-u(x-\Delta)}{2\Delta} = u'(x) - \frac{\Delta^2}{6}u^{(3)}(x) + O(\Delta^4)$$

To control high-wave number noise, a spatial gaussian filler is tested to the displacement before taking spatial derivative. For the spatial-derivative estimates, applying Gaussian smoothing with σ ≈ 0.75–1.0 (in grid-cell units) reduces the MSE at Δ/λS = 0.25 to below that at Δ/λS = 0.50.

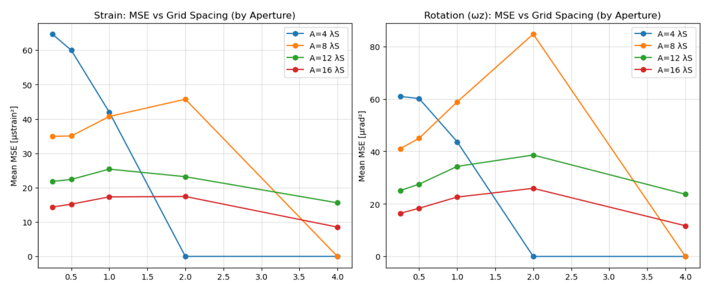

In terms of the sensitivity to the high-wavenumber noise filtering, ω has more sensitive than ε.

c) Physical insights: near-irrotational nature of far-field P; dominance of rotation in S and in- duction (near-field) terms; free-surface effects on vertical rotation.
Rotation tensor doesn't be observed at the first P-wave arrival in this near-irrotational far-field P wave scheme. Far field S term and Near field term has A**n**, which is perpendicular to radiation direction and $1/r^n$ generates spatial gradient, then dominant rotations.
On the assumption of the free-surface considering $\sigma_{iz} = 0$, even far-field P term cause vertical rotation via reflection and phase shift.

d) Practical implications for strainmeters, rotational seismometers, and DAS; recommended design rules (e.g., Δ/λS targets).
Recommended designs are $A/\lambda_S \geq 12\ to\ 16$ and $\Delta/\lambda_S \approx$ 0.25–0.5, which balance truncation error and noise amplification in spatial differencing. For $\lambda_S \approx$ 1.3km, $A/\lambda_S = 16$ (this study), implies an array of 20.8 × 20.8km. The required sensor count at $\Delta/\lambda_S = 0.25$ would be impractical for rotational seismometers, but DAS can feasibly realize this dense sampling, noting it measures axial strain only and demands careful filtering and geometry to recover shear/rotation.
A hybrid deployment is therefore advisable: place a small cluster of strainmeters and a few rotational seismometers near the array center (or anticipated sources) to constrain near-field and intermediate terms, while covering the broader aperture with DAS to capture long-wavelength structure and provide dense spatial gradients.